Alterations in Hepatic Fructose Metabolism in Cirrhotic Patients Demonstrated by Dynamic ^{31}Phosphorus Spectroscopy

JEAN-FRANÇOIS DUFOUR,[1] CHRISTOPHER STOUPIS,[2] FRANÇOIS LAZEYRAS,[2] PETER VOCK,[2] FRANÇOIS TERRIER[2] AND JÜRG REICHEN[1]

Departments of [1]Clinical Pharmacology and [2]Radiology, University of Berne, CH 3010 Berne, Switzerland

Quantitative liver function tests are based on the clearance concept and measure the plasma disappearance of a test compound such as galactose. Metabolism is inferred to be predominantly hepatic, and usually no knowledge is obtained of the true time course of metabolite formation. Dynamic ^{31}phosphorus magnetic resonance spectroscopy after intravenous administration of fructose directly measures hepatic sugar metabolism. To determine the feasability and the utility of ^{31}P magnetic resonance spectroscopy, we studied the responses of six healthy subjects and nine patients with nonalcoholic cirrhosis to a fructose load. Results were related to the impairment of hepatic function assessed by the galactose-elimination capacity test. Liver spectra were acquired in a 1.5 T whole-body nuclear magnetic resonance unit with a surface coil (9-cm diameter) placed ventrally on the liver; the one-dimensional chemical-shift imaging technique was used to obtain spectra from tissue slices parallel to the surface coil. After a basal spectrum had been obtained, fructose (250 mg/kg) was injected intravenously, and further spectra were collected sequentially every 6 min for 1 hr. Formation of monophosphate esters (9% ± 5% vs. 20% ± 8% of total area; p < 0.01) and utilization of inorganic phosphate (5% ± 4% vs. 11% ± 3% of total area; p < 0.005) were markedly decreased in cirrhotic patients. These measures correlated with the severity of the impairment of liver function measured by the galactose-elimination capacity (r = 0.53 to 0.69; p < 0.05). We conclude that dynamic ^{31}P magnetic resonance spectroscopy is a safe, clinically feasible test that allows detailed insights into biochemical events in liver disease. (HEPATOLOGY 1992; 15:835-842.)

Quantitation of liver function is necessary to assess the degree of liver impairment, to objectively evaluate response to treatment and to select transplant recipients (1). Most of the commonly used quantitative tests, such as galactose-elimination capacity (2), sulfobromophthalein clearance (3) or antipyrine clearance (4) measure the disappearance of a test compound from blood. From these measurements, clearance is calculated and functional capacities are inferred without knowledge of details of the hepatic metabolism. Moreover, in all these tests one assumes extrahepatic metabolism to be negligible or absent.

Magnetic resonance spectroscopy (MRS) has considerable potential for assessing metabolism directly in vivo, noninvasively and in real time (5). The liver is a voluminous, homogeneous organ close to the body surface; these characteristics make it well suited for investigation by MRS. In particular, by means of ^{31}phosphorus MRS (^{31}P-MRS), one can determine the relative concentration of ATP, inorganic phosphate (P_i), phosphomonoesters (PMEs) and phosphodiesters (PDEs) (6); furthermore, intracellular pH (pH_i) can be calculated from the chemical shift of P_i (7).

In dynamic ^{31}P-MRS, an intravenous load of fructose stresses liver metabolism, inducing an accumulation of PMEs (mainly fructose-1-phosphate), consumption of ATP and a drop in liver P_i, which is followed by a rise overshooting its initial value (8, 9). In a previous study, we described dose-response curves of these metabolic modifications induced by fructose in the normal human liver (9). The aim of this study was to determine whether dynamic ^{31}P-MRS can detect biochemical abnormalities in the livers of patients with cirrhosis, and to correlate these findings with an established indicator of severity of the disease (namely, the galactose elimination capacity [2, 10]).

MATERIALS AND METHODS

Subjects. The studies were performed in six healthy volunteers and nine patients with cirrhosis of nonalcoholic origin. The characteristics of these subjects are summarized in Table 1. Diagnosis was confirmed by liver biopsy in all but Patient 13. Liver function was characterized by the Child-Pugh classification and by the galactose-elimination capacity. Galactose-elimination testing was performed within 3 mo of the spectroscopy study after an intravenous load of galactose (0.5 gm/kg) was administered according to the method described by

TABLE 1. Characteristics of the normal volunteers and the cirrhotic patients

Subject	Age	Sex	GEC	CPC	Diagnosis
1	25	M	ND	—	Normal volunteer
2	29	M	7.1	—	Normal volunteer
3	29	M	7.4	—	Normal volunteer
4	33	F	7.2	—	Normal volunteer
5	38	M	6.1	—	Normal volunteer
6	44	M	8.1	—	Normal volunteer
Mean ± 1 S.D.	33 ± 7	—	7.2 ± 0.7	—	—
7	23	M	3.0	13	Cryptogenic cirrhosis
8	29	F	4.7	6	Autoimmune hepatitis
9	35	M	3.2	7	Chronic hepatitis B
10	45	M	3.9	6	Cryptogenic cirrhosis
11	54	M	4.9	7	Chronic hepatitis B and C
12	57	M	5.1	5	Chronic hepatitis B
13	58	F	3.5	9	Chronic hepatitis C
14	61	F	3.0	10	Autoimmune hepatitis
15	70	F	3.0	6	Cryptogenic cirrhosis
Mean ± 1 S.D.	47 ± 16	—	3.8 ± 0.9[a]	—	—

GEC = galactose-elimination capacity; CPC = Child-Pugh class; ND = not determined.
[a]$p < 0.001$ compared to controls.

Tygstrup (2), with modifications described from this department (11). The study was approved by the Ethics Committee of the Faculty of Medicine. Each subject gave informed consent.

Experimental Design. After a basal spectrum had been obtained, fructose (250 mg/kg) was rapidly injected intravenously (time 0); further spectra were then collected sequentially every 6 min for 1 hr; 4 min were used for data acquisition and 2 min were spent in data transfer. Thus 10 spectra after fructose injection were obtained at 4, 10, 16, 22, 28, 34, 40, 46, 52 and 58 min. For technical reasons, two patients had only six spectra and one patient had only five spectra (patients 10, 13 and 14).

^{31}P-MRS. All measurements were performed at 1.5 T on a General Electric Signa system (General Electric Corp., Milwaukee, WI). A 9-cm-diameter double-tuned surface coil was used both for shimming and ^{31}P-MRS. Shimming was performed on the whole sensitive volume of the surface coil with the water line. The line-width achieved was less than 0.5 ppm. The ^{31}P radiofrequency field strength was adjusted to minimize the phosphocreatine (PCr) peak in a nonlocalized experiment. A one-dimensional chemical-shift method was used for the localization (12), with the following parameters: spectral width, ± 1,000 Hz; number of complex data points, 256; recycle time, 1 sec; and 64 phase-encoding steps with four acquisitions per step giving a total acquisition time of 4 min and 16 sec. The phase-encoding gradient was 0.5 msec, and its amplitude was set to accommodate a slice thickness of 2 cm. The preacquisition delay was 0.5 msec, corresponding to one dwell period. The excitation pulse width was 400 μsec.

Analysis of Spectra. Data were processed on a remote data station (Nicolet, Fremont, CA). They were apodized with an exponential multiplication corresponding to 10 Hz line broadening in the chemical-shift dimension, followed by zero filling. No apodization was made in the spatial dimension. After a two-dimension Fourier transformation, the spectra corresponding to the liver region were zero and first-order phase-corrected for the one-dwell-period acquisition delay. No baseline correction was performed. To measure the area under each peak, a manual line-fitting routine assuming purely lorentzian line shape was used (CSICAP on our Nicolet station).

At a recycle time of less than five times T1, spectra were acquired under partially saturating conditions. Knowing T1, one can evaluate the effect of saturation on peak intensities. From T1 data published in the literature (namely, 0.41 ± 0.10 sec for P_i, 1.4 ± 0.1 sec for PDE, 0.68 ± 0.09 sec for α-ATP, 0.40 ± 0.13 sec for β-ATP and 0.43 ± 0.18 sec for γ-ATP [13]) or obtained in our laboratory (β-ATP 0.35 msec measured in two normal volunteers with an inversion recovery sequence combined with depth-resolved surface-coil spectroscopy [DRESS]), one can calculate the saturation for each peak at a recycle time of 1 sec. The signals from P_i and β-ATP were relaxed to more than 90%, whereas PDE was about 50% of its unsaturated density. The saturation of PME was intermediate between PDE and β-ATP. We did not feel that correction for saturation was needed because (a) the recycle time was the same for each experiment, permitting direct comparison of spectra, and (b) we were more interested in relative changes of peak intensities rather than their absolute values.

Besides decreasing acquisition time, a short recycle time has two further advantages. Because phosphorus metabolites have a much longer T1 in muscle than in liver (13), signals from thoracic and abdominal wall muscles are selectively saturated, thereby reducing contamination of liver spectra. Moreover, contamination by abdominal and thoracic wall muscle was continuously corrected for with the PCr peak (representing only muscle) as described previously (9). Contamination was less than 10% for the β-ATP peak. Moreover, resolution of liver P_i is enhanced with a short recycle time because the adjacent PME and PDE peaks are more strongly saturated because of their longer T1s. This facilitates measurement of pH (14).

Data Analysis and Presentation. The total area of spectrum represents the amount of signal received from all ^{31}P atoms in the probed volume; this was taken as 100%. Individual peaks will be reported as the percentage of the total area. The means of these relative areas were plotted against time; to compare serial measurements between normal volunteers and cirrhotic

patients, the following summary measurements were obtained (15).

The peak response in PME formation was calculated as

$$\Delta PME = PME_{max} - PME_0 \qquad (1)$$

where ΔPME is expressed as the change in relative area (%) and the subscripts max and 0 refer to the relative PME area at its maximal value after fructose administration and the initial value, respectively. The velocity of PME formation (v_{PME}; expressed as relative area, %/min) was calculated as

$$v_{PME} = (PME_4 - PME_0)/4 \qquad (2)$$

where the subscripts 4 and 0 refer to the relative area of PME 4 min after fructose administration and at baseline, respectively.

The amplitude of the P_i (relative area in %) response was calculated as

$$\Delta P_i = P_{i_{min + 12}} - P_{i_{min}} \qquad (3)$$

where the subscript min stands for the minimal value of the relative P_i peak area after fructose administration and $_{min + 12}$ refers to the relative area observed 12 min thereafter. The velocity of P_i utilization (vP_i) was calculated in a fashion analogous to that for PME formation with equation 2.

Changes in the relative contribution of ATP were calculated with the β-ATP peak because this peak represents ATP only (16), whereas the α-ATP and γ-ATP peaks contain information about ADP and NAD (17). Contamination of hepatic β-ATP with muscle ATP was corrected with the PCr peak as described previously (9). ATP utilization (relative area, in %) was calculated as ΔATP:

$$\Delta ATP = ATP_0 - ATP_{min} \qquad (4)$$

where the subscripts 0 and min refer to the relative ATP peak area at baseline and at its minimal value after fructose administration, respectively. Velocity of ATP utilization (relative area in %/min) was calculated as

$$v_{ATP} = (ATP_{min + 6} - ATP_{min})/6 \qquad (5)$$

where the subscript min stands for the minimal value of the relative ATP peak area after fructose administration and $min + 6$ represents the value observed 6 min thereafter. The time intervals in equations 2, 3, and 5 were chosen because it was found that the PME, P_i and ATP area, respectively, exhibited the most marked changes at the time points in equations 2, 3, and 5.

pH_i of the liver was derived from the chemical shift of P_i according to the following equation:

$$pH_i = 6.75 + log[(d - 3.27)/(5.78 - d)] \qquad (6)$$

where d is the chemical shift of the P_i peak in parts per million (7). With a repetition time of 1 sec, the contribution of the extracellular P_i is negligible because the relaxation time (T1) of the intracellular P_i is of the order of 400 msec, whereas that of blood is 3 sec (17). We used the α-ATP peak as a reference frequency, assigning it a chemical shift of -7.55 (18). Accurate pH determination depends on (a) measuring the chemical shift of P_i and (b) relating the P_i shift to pH. Possible sources of error include baseline fluctuations, peak overlap, line-broadening due to field inhomogeneities, poor signal-to-noise
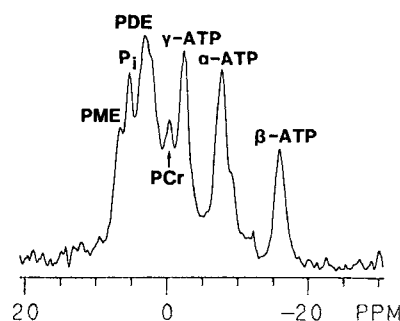

FIG. 1. 31P spectrum of a normal volunteer (Subject 2).

ratio and calibration uncertainties. For individual measurements, the uncertainty in pH ranges from 0.05 to 0.15 pH units (19). Measurements of relative changes in pH remove some systematic errors; thus they are more accurate than absolute pH values.

All data are expressed as mean ± 1 S.D. The statistical differences between the means of the summary measures were evaluated by Student's t test (20). The effects of fructose in the same subjects were compared with the result of the paired t test (20). Linear-regression analysis was performed by the method of least squares (20). Statistical significance was set at $p < 0.05$.

RESULTS

In each subject, spectra with adequate suppression of signals from surface tissues and distinguishable peaks could be obtained (Fig. 1). Comparisons of the basal spectra between the healthy and cirrhotic subjects are described in Table 2. The P_i and the PME and the ATP peaks had comparable relative areas in both groups. The contribution of PDE was significantly smaller in cirrhotic patients than in healthy subjects (33% ± 5% vs. 38% ± 5%; $p < 0.05$).

Figure 2A shows the changes induced by a fructose load on the 31P spectrum in a normal volunteer; the changes seen in a cirrhotic patient are shown for comparison in Figure 2B. The relative areas of the different compounds after fructose administration are reported in Table 2. Only values up to 28 min are reported because thereafter no further significant changes were observed.

The time course of PME is shown in Figure 3. In both groups the relative area of PME increased in response to the fructose load. It can be seen that the increase was more marked in normal volunteers than in patients with liver disease; indeed, ΔPME averaged 20% ± 8% and 9% ± 5% in controls and cirrhotics, respectively ($p < 0.01$). The velocity (v_{PME}) was faster in normal subjects than in cirrhotic patients (3.2 ± 1.4 vs 1.8 ± 1.4%/min; $p < 0.05$). ΔPME correlated with the galactose elimination capacity ($r = 0.648$, $p < 0.01$; Fig. 4). Similarly, the velocity correlated with galactose-elimination capacity ($r = 0.531$, $p < 0.05$; data not shown).

The time course of P_i after the fructose load is shown in Fig. 5. In both groups, P_i initially fell in response to the fructose load; thereafter an increase overshot the
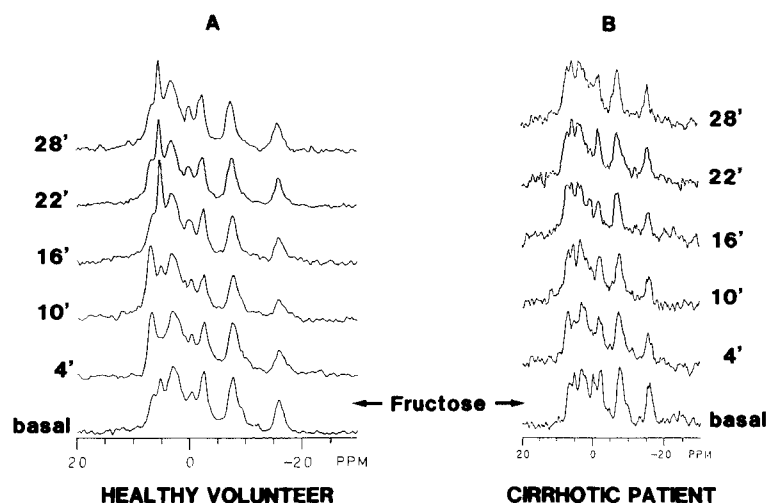
FIG. 2. Time course of ^{31}P-MRS spectra of a normal volunteer (Subject 2) (A) and of a cirrhotic patient (Subject 11) (B) before and after intravenous fructose loads (250 mg/kg). A fructose-induced increase in the PME peak, with a concomitant decrease in P_i and ATP, can be seen.

TABLE 2. Relative areas of the different ^{31}P-metabolites before and at the indicated times after a fructose load in normal volunteers and patients with cirrhosis

| Metabolite | \multicolumn{6}{c}{Time after fructose load (min)} | | | | | |
	0	4	10	16	22	28
PME						
Control	$8 \pm 3^{a, b}$	21 ± 5	24 ± 13	16 ± 8	14 ± 4	12 ± 5
Cirrhotic	7 ± 3	14 ± 5	13 ± 6	12 ± 5	11 ± 3	10 ± 3
PDE						
Control	38 ± 5	40 ± 4	35 ± 6	35 ± 6	35 ± 5	37 ± 7
Cirrhotic	33 ± 5	33 ± 5	34 ± 5	32 ± 6	31 ± 7	29 ± 8
P_i						
Control	7 ± 3	1 ± 1	4 ± 4	9 ± 6	11 ± 3	11 ± 3
Cirrhotic	5 ± 1	3 ± 2	5 ± 2	8 ± 3	8 ± 3	8 ± 3
β-ATP						
Control	9 ± 1	6 ± 1	6 ± 2	7 ± 3	5 ± 2	6 ± 3
Cirrhotic	10 ± 2	8 ± 2	7 ± 2	8 ± 3	9 ± 3	7 ± 2
pH_i						
Control	7.21 ± 0.10	7.31 ± 0.18	7.32 ± 0.25	7.42 ± 0.32	7.43 ± 0.30	7.35 ± 0.08
Cirrhotic	7.19 ± 0.13	7.21 ± 0.21	7.25 ± 0.12	7.21 ± 0.15	7.25 ± 0.15	7.27 ± 0.23

The fructose load was 250 mg/kg. pH_i was calculated with α-ATP as a chemical shift reference.
[a]Data expressed as mean $\pm$ 1 S.D.
[b]All values except pH_i are expressed as percentage of total area.

initial value. In healthy volunteers, P_i fell to 14% of its basal value (from 7% $\pm$ 3% to 1% $\pm$ 1%; p < 0.002). Thereafter an overshoot to 157% (11% $\pm$ 3%) was seen. In cirrhotic patients, in contrast, P_i fell only to 60% of its initial value (from 5% $\pm$ 1% to 3% $\pm$ 2%; p < 0.01) and overshot to 160% (8% $\pm$ 3%). Thus the magnitude of the P_i movement was significantly different between the two groups; the corresponding amplitudes (ΔP_i) averaged 11% $\pm$ 3% and 5% $\pm$ 4% in healthy volunteers and in cirrhotic patients, respectively (p < 0.005). ΔP_i correlated with the galactose-elimination capacity (r = 0.691, p < 0.01; Fig. 6). P_i decreased faster in normal subjects than in cirrhotic patients (vP_i, -1.46 ± 0.67 vs. -0.57 ± 0.57%/min; p < 0.01); it also correlated with

the galactose-elimination capacity (r = -0.686; p < 0.01; data not shown).

Figure 7 shows the time course of the β-ATP corrected for the muscle contamination. Fructose load induced significant ATP utilization in both groups: β-ATP fell to 66% of its basal value in healthy volunteers (from 9% $\pm$ 1% to 6% $\pm$ 1%; p < 0.01) but only to 80% in cirrhotic patients (from 10% $\pm$ 2% to 8% $\pm$ 2%; p < 0.01). The magnitude of β-ATP consumption was not different between the normal subjects and the cirrhotic patients; ΔATP averaged 4.1% $\pm$ 1.6% and 4.3% $\pm$ 3.2% (p = not significant). Thereafter ATP increased again because of resynthesis but did not return to its basal value during the 1-hr observation period. The
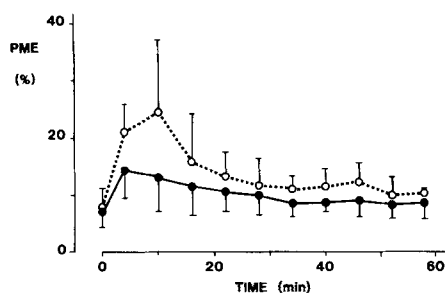
FIG. 3. Evolution of PMEs induced by a fructose load in normal volunteers (○) and cirrhotic patients (●). PMEs are expressed as percentage of the total area. Mean ± 1S.D. is given.
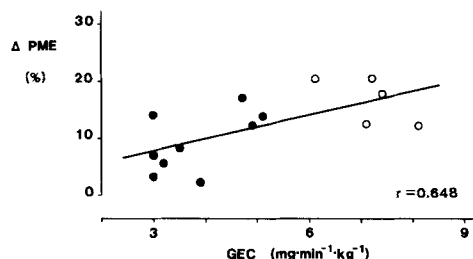

FIG. 5. Evolution of inorganic phosphorus after an intravenous fructose load in normal volunteers (○) and cirrhotic patients (●). P_i is expressed as percentage of total area; mean ± 1 S.D. is given.

FIG. 4. Relationship between galactose elimination capacity *(GEC)* and the maximal increase in the PME peak induced by fructose in normal volunteers (○) and cirrhotic patients (●). The two parameters were significantly correlated; the regression equation was $y = 1.45 + 2.08 \cdot x$ ($r = 0.648$, $p < 0.01$).

FIG. 6. Relationship between galactose elimination capacity *(GEC)* and the maximal amplitude of P_i (ΔP_i) in normal volunteers (○) and cirrhotic patients (●). The two parameters are significantly correlated; the regression equation was $y = 1.703 \cdot x - 1.281$ ($r = 0.691$; $p < 0.01$).

velocity of ATP synthesis was not different between the two groups (0.42 ± 0.48 vs. $0.42 \pm 0.20\%$/min; p = not significant).

Basal intracellular pH was similar in normal volunteers and in cirrhotic patients (Table 2). The fructose load induced a trend toward alkalinization in normal volunteers, but this effect was not statistically significant (Fig. 8).

The intensity of the PCr peak varied from one spectrum to the next because slight movements of the subject influenced the efficiency of suppression of the muscle signal. Means of the maximum of changes of PCr relative areas during the time course were 7% ± 5% and 5% ± 3% in controls and cirrhotics, respectively; p = not significant).

The fructose injections were tolerated well by normal volunteers and cirrhotic subjects. In particular, no episodes of hypoglycemia were noted. Seven of the subjects experienced mild, deep epigastric pain during the first 10 min after the injection, but the pain did not necessitate any changes in the experimental protocol.

DISCUSSION

Dynamic ^{31}P-MRS demonstrated metabolic liver abnormalities in response to a fructose load (namely, decreased PME formation and P_i utilization) in patients with nonalcoholic cirrhosis. These changes correlated with a classical clearance test of liver function, the galactose-elimination capacity. All relevant infor-
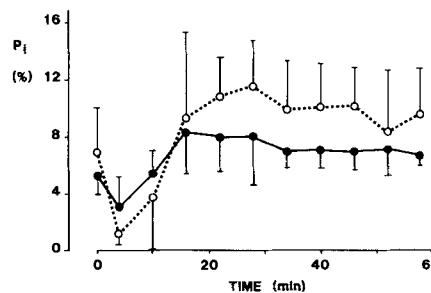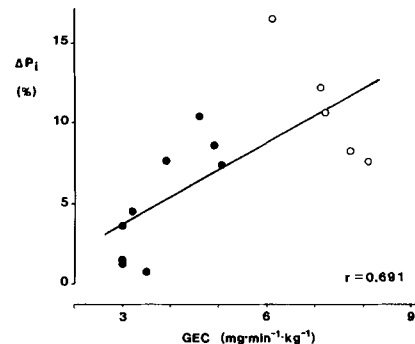
mation could be obtained during the first 30 min of the test.

The contribution of the different ^{31}P metabolites in the basal spectra was similar to that reported by Schilling et al. (21). The lack of a difference in the relative contribution of PME, P_i and β-ATP to total ^{31}P metabolites was in agreement with a recent study in cirrhotic patients (22). The only significant difference we found between cirrhotic patients and healthy volunteers was a decrease in PDE in cirrhotic patients; this phenomenon was first described by Meyerhoff et al. (23). The PDE signal in our spectra is only hepatic in origin (24); its different components have not yet been conclusively elucidated. In the perfused rat liver, the PDE signal has been ascribed to phospholipid breakdown products such as glycerophosphocholine and glycerophosphoethanolamine (25). However, according to a more recent study in rats (26), it has been ascribed to phospholipid bilayers. The main difference between these studies was the field strength; the lower field strength used by Murphy et al. (26) permits better visualization of signals from the phospholipid bilayer. Because in liver the endoplasmic reticulum comprises most phospholipid membranes, it is tempting to speculate that the observed decrease in PDE indicates a reduction in endoplasmic reticulum.
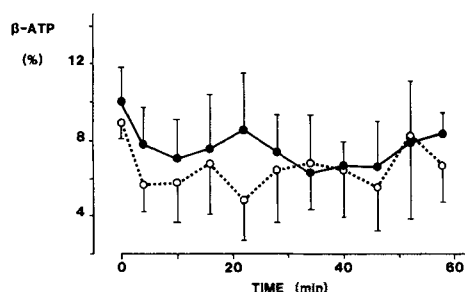
FIG. 7. Evolution of β-ATP after intravenous fructose loading in normal volunteers (○) and cirrhotic patients (●). β-ATP is expressed as percentage of total area; mean ± 1 S.D. is given.
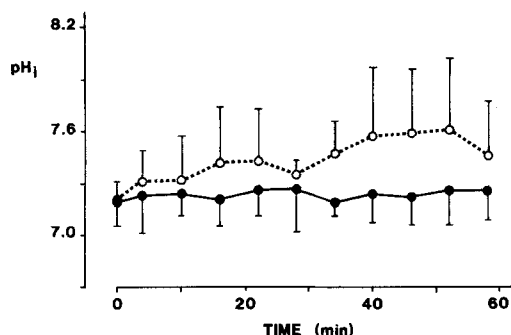

FIG. 8. Evolution of pH_i after intravenous fructose loading (250 mg/kg) in normal volunteers (○) and cirrhotic patients (●). pH_i was calculated with the chemical shift of P_i, with α-ATP as reference peak. For further methodological details, see "Subjects and Methods." Fructose did not significantly affect pH_i in either group.

Our results were expressed as relative areas; thus they do not represent tissue concentrations, but a distribution of ^{31}P atoms that is dependent on biochemical environment. Absolute quantification is not possible with the techniques used in this investigation because of the use of a surface coil and the choice of localization techniques. Absolute quantification was recently made possible with calibration with aqueous standard solutions; using this technique, Meyerhoff et al. were able to demonstrate a significant decrease of absolute hepatic ^{31}P metabolites (25% to 50%, expressed in mmol/kg wet wt) in cirrhotic patients compared with normal subjects (23). In our case, absolute quantitation was made difficult for the following reasons: the flip angle was not set with the help of an external reference but by minimizing the PCr peak and varied from one experiment to another. The localized slice was not necessarily parallel to the surface coil, making computation of the B1 field plot more difficult. Finally, the heterogeneity of the liver, certainly increased in cirrhotic patients, was not assessed. Nevertheless, our method is well suited to quantitatively follow relative changes induced by a metabolic stress such as a fructose load. The response of the different hepatic ^{31}P metabolites to fructose in the healthy volunteers is in agreement with results obtained in previous biochemical and nuclear magnetic resonance investigations (8, 9, 17, 27, 28).

The more pronounced increase in PME in normal subjects than in cirrhotic patients indicates that normal liver phosphorylates fructose more efficiently than does cirrhotic liver. Decreased use of fructose in parenchymal liver disease has also been reported with a [^{14}C]fructose breath test (29).

Many compounds with phosphorylated sugar residues contribute to the PME peak, but after a fructose load the increase of PME is caused mainly by formation of fructose-1-phosphate (30). The cleavage of fructose-1-phosphate by liver aldolase B is inhibited by several phosphorylated intermediates, in particular inosine monophosphate (28). After fructose loading, inosine monophosphate accumulates in liver in connection with the hepatic depletion of adenine nucleotides (31). The PME response correlates with galactose-elimination capacity, which measures the capacity to phosphorylate the galactose (2).

The depletion of P_i is a consequence of the fixation of phosphate in phosphorylated intermediates and in re-synthesized ATP (32); the overshoot in P_i content of the liver after this transient drop results from dephosphorylation of high-energy phosphates and from influx of P_i from the blood (28, 33). Both magnitude and velocity of this P_i movement were significantly reduced in cirrhotic liver compared with normal liver, reflecting diminished fructose metabolism.

The sustained reduction in the β-ATP is related to its utilization by fructokinase and to the depletion of P_i, which limits the regeneration of ATP. A more pronounced depression of hepatic ATP content has been described with use of fructose infusions (8) rather than the bolus injection used in this study; a larger dose of fructose can also further deplete hepatic ATP (9). The decreased phosphorylation of fructose in cirrhotic patients imposes less of a demand on ATP synthesis; whether a relatively larger dose of fructose could have made apparent a defect in ATP synthesis rate as described in human cirrhosis (34) remains to be investigated.

With the α-ATP peak as an internal chemical-shift reference, the basal pH showed no difference between normal volunteers and cirrhotic patients (7.21 ± 0.49 vs. 7.19 ± 0.13). These results are consistent with previous ^{31}P-MRS studies in human liver. Thus Oberhänsli et al. measured a mean pH_i of 7.24 ± 0.01 in 11 normal volunteers (6) and Schilling et al. found a mean value of 7.3 ± 0.1 in 10 normal volunteers (21). The influence of liver disease on pH_i is controversial. Although Meyerhoff et al. found a lower pH_i in patients with alcoholic liver disease (23), Angus et al. could not reproduce this finding (35). After fructose loading in normal volunteers, an initial decrease of pH_i followed by intracellular alkalinization was found (36); unfortunately, the reference peak in this study was not indicated. The initial acidification can be explained biochemically because fructose metabolism produces protons during the formation of fructose-1-phosphate and later during its transformation to lactate (37). The subsequent alkalinization is more difficult to under-

stand but could represent an overshoot in compensation for the initial drop in pH_i.

In this study, however, we observed only a trend toward alkalinization in normal volunteers, but not cirrhotic patients. Further investigations into the effect of fructose loading on pH are clearly warranted because fructose can induce lactate formation. This could lead to lactic acidosis in cirrhotic patients because their ability to clear lactate is diminished (38). A crucial point will be the selection of an adequate chemical-shift reference. Indeed, the ATP peak appears less suitable than the water resonance from the proton spectrum used for shimming because their shift depends not only on changes in pH but could also be altered by changes in intrahepatic magnesium concentrations; furthermore, they are broadened by the presence of other resonances (19).

Our studies were performed on subjects in the fed state. This may permit better visualization of the PME response to fructose because in the fed state, glucose release through fructose-1-phosphate degradation is inhibited (39). Other investigators have performed fructose-loading experiments on subjects in the fasted state (8); this could also account for part of the discrepancy in the effects of fructose loading on hepatic ATP (vide supra).

The diminished metabolism of fructose in cirrhotic livers could be due to reduced liver uptake, to impaired hepatic phosphorylation or to both. The blood half-life of fructose is only marginally prolonged in cirrhosis (33); similarly, intravenous fructose-tolerance tests in patients with hepatitis and cirrhosis also demonstrate normal fructose uptake in liver disease (40, 41). Thus the diminished metabolism of fructose is probably due to impaired hepatic metabolism rather than to reduced transport of fructose into hepatocytes. The correlation with galactose-elimination capacity, where the rate-limiting step is not uptake but phosphorylation (2), further supports this contention.

Our results do not permit identification of the reason(s) for the decreased metabolism of fructose (in particular, whether this is due to a decreased cell number or a decreased enzyme or substrate [ATP] content of individual hepatocytes). As one would anticipate, the volume fraction of hepatocytes is decreased in animal models of cirrhosis, but total liver cell mass can long be maintained (42). Defects in mitochondrial ATP content have been described (34), but in the whole organ different strategies to overcome these in vitro defects have been described by our group (43; Krähenbühl S, Reichen J, Unpublished observations).

Intravenous injection of fructose is not without risk. Fructose infusion in patients with liver diseases can induce severe lactic acidosis (44). Another risk is hypoglycemia, which can be induced not only in patients with hereditary fructose intolerance but also in healthy adults (45). As in our previous work, we encountered no major problems; the only adverse effect noticed was mild and transient epigastric pain in half the cases (9).

In conclusion, dynamic ³¹P-MRS after an intravenous fructose load permits safe and relatively rapid functional evaluation of hepatic sugar and phosphate metabolism. Whereas a classical clearance test such as the galactose-elimination capacity describes only clearance from blood, dynamic ³¹P-MRS describes metabolic pathways with a reduction of sugar phosphorylation and of P_i utilization. Dynamic ³¹P-MRS permits better understanding of physiological and pathological metabolic mechanisms.

REFERENCES

1. Bircher J. Quantitative assessment of deranged hepatic function: a missed opportunity? Semin Liver Dis 1983;3:275-284.
2. Tygstrup N. Determination of the hepatic galactose elimination capacity after a single intravenous injection in man. Acta Physiol Scand 1963;58:162-172.
3. Haecki W, Bircher J, Preisig R. A new look at the plasma disappearance of sulfobromophthalein (BSP): correlation with the BSP transport maximum and the hepatic plasma flow in man. J Lab Clin Med 1976;88:1019-1031.
4. Andreasen PB, Ranek L, Statland BE, Tygstrup N. Clearance of antipyrine: dependence of quantitative liver function. Eur J Clin Invest 1974;4:129-134.
5. Gadian DG. Nuclear magnetic resonance and its applications to living systems. New York: Oxford University Press, 1982.
6. Oberhänsli RD, Galloway GJ, Hilton-Jones D, Bore P, Styles P, Rajagopolan B, Taylor DJ, et al. The study of human organs by phosphorus-31 topical magnetic resonance spectroscopy. Br J Radiol 1987;60:367-373.
7. Seo Y, Murakami M, Watari H, Imai Y, Yoshizaki K, Nishikawa H, Morimoto T. Intracellular pH determination by a ³¹P-NMR technique: the second dissociation constant of phosphoric acid in a biological system. J Biochem 1983;94:729-734.
8. Oberhaensli RD, Galloway GJ, Taylor DJ, Bore PJ, Radda GK. Assessment of human liver metabolism by phosphorus-31 magnetic resonance spectroscopy. Br J Radiol 1986;59:695-699.
9. Terrier F, Vock P, Cotting J, Ladebeck R, Reichen J, Hentschel D. Effect of intravenous fructose on the P-31 MR spectrum of the liver: dose response in healthy volunteers. Radiology 1989;171:557-563.
10. Bircher J, Blankart R, Halpern A, Haecki W, Laissue J, Preisig R. Criteria for assessment of functional impairment in patients with cirrhosis of the liver. Eur J Clin Invest 1973;3:72-85.
11. Heri M, Bircher J. Die Galaktose-eliminationskapazitaet, ein zuverlaessiger Test zur quantitativen Erfassung der Leberfunktion. Schweiz Med Wochenschr 1971;101:735-736.
12. Brown TR, Kincaid BM, Urgubil K. NMR chemical shift imaging in three dimensions. Proc Natl Acad Sci USA 1982;79:3523-3526.
13. Buchtal SD, Thoma WJ, Taylor JS, Nelson SJ, Brown TR. In vivo T1 values of phosphorus metabolites in human liver and muscle determined at 1.5 T by chemical shift imaging. NMR Biomed 1989;2:298-304.
14. Cox IH, Coutts GA, Gadian DG, Ghosh P, Sargentoni J, Young IR. Saturation effects in phosphorous-31 magnetic resonance spectra of the human liver. Magn Reson Med 1991;17:53-61.
15. Matthews JNS, Altman DG, Campbell MJ, Royston P. Analysis of serial measurements in medical research. Br Med J 1990;300:230-235.
16. Helzberg JH, Brown MS, Smith DJ, Gore JC, Gordon ER. Metabolic state of the rat liver with ethanol: comparison of in vivo ³¹phosphorus nuclear magnetic resonance spectroscopy with freeze clamp assessment. HEPATOLOGY 1987;7:83-88.

17. Iles RA, Stevens AN, Griffiths JR, Morris PG. Phosphorylation status of liver by ³¹P-NMR spectroscopy and its implications for metabolic control. Biochem J 1985;229:141-151.

18. Koretsky AP, Wang S, Murphy-Boesch J, Klein MP, James TL, Weiner MW. ³¹P NMR spectroscopy of rat organs, in situ, using chronically implanted radiofrequency coils. Proc Natl Acad Sci USA 1983;80:7491-7495.

19. Madden A, Leach MO, Sharp JC, Collins DJ, Easton D. A quantitative analysis of the accuracy of in vivo pH measurements with ³¹P-NMR spectroscopy: assessment of pH measurement methodology. NMR Biomed 1981;4:1-11.

20. Snedecor GW, Cochran WG. Statistical methods. Ames, IA: Iowa State University Press, 1967.

21. Schilling A, Gewiese B, Stiller D, Roemer T, Wolf KJ. Einfluss der Ernaehrungslage auf das ³¹P-MR-Spektrum der gesunden Leber. F Roentgenstr 1990;153:369-372.

22. Oberhänsli R, Rajagopalan B, Galloway GJ, Taylor DJ, Radda GK. Study of human liver disease with P-31 magnetic resonance spectroscopy. Gut 1990;31:463-467.

23. Meyerhoff DJ, Boska MD, Thomas AM, Weiner MW. Alcoholic liver disease: quantitative image-guided P-31 MR spectroscopy. Radiology 1989;173:393-400.

24. Dawson MJ. Quantitative analysis of metabolite levels in normal human subjects by ³¹P topical magnetic resonance. Biosci Rep 1982;2:727-733.

25. Cohen SM. Simultaneous ¹³C and ³¹P NMR studies of perfused rat liver: effects of insulin and glucagon and a ¹³C NMR assay of free Mg. J Biol Chem 1983;258:14294-14308.

26. Murphy EJ, Rajagopalan BR, Brindle KM, Radda GK. Phospholipid bilayer contribution to ³¹P-NMR spectra in vivo. Magn Reson Med 1989;12:282-289.

27. Griffiths JR, Stevens AN, Gadian DG, Iles RA, Porteus R. Hepatic fructose metabolism studied by ³¹P nuclear magnetic resonance in the anesthetized rat. Biochem Soc Trans 1980;8:641.

28. Woods HF, Eggleston LV, Krebs HA. The cause of hepatic accumulation of fructose-1-phosphate on fructose loading. Biochem J 1970;119:501-510.

29. Krönert E, Herzog M, Wolf P. Die unterschiedliche Verwertung ¹⁴C-markierter Glukose und Fruktose bei Lebergesunden und Leberkranken. Med Ernährung 1969;10:31-32.

30. Kjerulf-Jensen K. The phosphate esters formed in the liver tissue of rats and rabbits during assimilation of hexosis and glycerol. Acta Physiol Scand 1942;4:249-258.

31. Maenpaeae P, Raivio K, Kekomaeki M. Liver adenine nucleotides:

32. Bode JC, Zelder O, Rumpelt HJ, Wittkamp U. Depletion of liver adenosine phosphates and metabolic effects of intravenous infusion of fructose or sorbitol in man and in the rat. Eur J Clin Invest 1973;3:436-441.

33. Smith LH, Ettinger RH, Seligson D. A comparison of the metabolism of fructose and glucose in hepatic disease and diabetes mellitus. J Clin Invest 1953;32:273-282.

34. Diaz Gil J, Rossi I, Escartin P, Segovia JM, Gosalvez M. Mitochondrial functions and content of microsomal and mitochondrial cytochromes in human cirrhosis. Clin Sci Mol Med 1977;52: 599-606.

35. Angus PW, Dixon RM, Rajagopalan B, Ryley NG, Simpson KJ, Peters TJ, Jewell DP, et al. A study of patients with alcoholic liver disease by ³¹P nuclear magnetic resonance spectroscopy. Clin Sci 1990;78:33-38.

36. Segebarth C, Grivegnee A, Luyten PR, Den Hollander JA. ¹H image-guided localized ³¹P MR spectroscopy of the human liver. Magn Res Biol Med 1988;1:7-16.

37. Iles RA, Griffiths JR, Stevens AN, Gadian DG, Porteous R. Effects of fructose on the energy status and acid-base status of the perfused starved rat liver. Biochem J 1980;192:191-202.

38. Mizock BA. Controversies in lactic acidosis. JAMA 1987;258: 497-501.

39. Sestoft L, Fleron P. Determination of the kinetic constant of fructose transport and phosphorylation in the perfused rat liver. Biochim Biophys Acta 1974;345:27-38.

40. Greence CH, Snell AM, Walters W. Diseases of the liver. I. A survey of tests of hepatic function. Arch Intern Med 1925;36:248-272.

41. Stewart CP, Scarborough H, Davidson JN. Some observations on the laevulose tolerance test. Q J Med 1938;7:229-261.

42. Reichen J, Egger B, Ohara N, Zeltner TB, Zysset T, Zimmerman A. Determinants of hepatic functions in liver cirrhosis in the rat: a multivariate analysis. J Clin Invest 1988;82:2069-2076.

43. Krähenbühl S, Reichen J, Zimmerman A, Stucki J. Mitochondrial structure and function in CCl₄-induced cirrhosis in the rat. HEPATOLOGY 1990;12:526-532.

44. Woods HF, Alberti KG. Dangers of intravenous fructose. Lancet 1972;2:1354-1357.

45. Felber JP, Renold AE, Zahnd GR. The comparative metabolism of glucose, fructose, galactose and sorbitol in normal subjects and in disease states. In: Hottiger A, Berger H, eds. Modern problems in pediatrics. vol. 4. Basel: Karger, 1959:467-489.

fructose-induced depletion and its effect on protein synthesis. Science 1968;161:1253-1254.